nature medicine

Modification of kidney barrier function by the urokinase receptor

Changli Wei[1], Clemens C Möller[1], Mehmet M Altintas[1], Jing Li[1], Karin Schwarz[2], Serena Zacchigna[3,4], Liang Xie[5], Anna Henger[6], Holger Schmid[7], Maria P Rastaldi[8], Peter Cowan[9], Matthias Kretzler[6], Roberto Parrilla[10], Moïse Bendayan[11], Vineet Gupta[1], Boris Nikolic[1], Raghu Kalluri[5], Peter Carmeliet[3,4], Peter Mundel[12] & Jochen Reiser[1]

Podocyte dysfunction, represented by foot process effacement and proteinuria, is often the starting point for progressive kidney disease. Therapies aimed at the cellular level of the disease are currently not available. Here we show that induction of urokinase receptor (uPAR) signaling in podocytes leads to foot process effacement and urinary protein loss via a mechanism that includes lipid-dependent activation of αvβ3 integrin. Mice lacking uPAR (*Plaur*$^{-/-}$) are protected from lipopolysaccharide (LPS)-mediated proteinuria but develop disease after expression of a constitutively active β3 integrin. Gene transfer studies reveal a prerequisite for uPAR expression in podocytes, but not in endothelial cells, for the development of LPS-mediated proteinuria. Mechanistically, uPAR is required to activate αvβ3 integrin in podocytes, promoting cell motility and activation of the small GTPases Cdc42 and Rac1. Blockade of αvβ3 integrin reduces podocyte motility *in vitro* and lowers proteinuria in mice. Our findings show a physiological role for uPAR signaling in the regulation of kidney permeability.

Proteinuria affects some 100 million people worldwide and is a feature of kidney dysfunction of glomerular origin; it is also a risk factor for both renal and extrarenal diseases[1]. Podocytes and their foot processes, together with endothelial cells and the glomerular basement membrane (GBM), are key components of the ultrafiltration system in the glomerulus (**Supplementary Fig. 1a** online). Podocytes are attached to the GBM via α3β1 integrin[2,3] and α and β dystroglycan[4]. Podocyte foot processes are interconnected by the slit diaphragm, a modified adherens junction[5]. Proteinuric kidney diseases are typically associated with foot process effacement and/or slit diaphragm disruption driven by a rearrangement of the podocyte microfilament system[6]. Recent work has advanced our understanding of the molecular framework underlying podocyte structure, largely through the analysis of hereditary proteinuria syndromes and genetic models[7]. A few studies also suggest mechanisms for the far more common acquired proteinuric diseases[8,9]. Despite this progress, there is a lack of cell-specific anti-proteinuric therapeutics. An emerging concept in the regulation of podocyte function is the regulation of the podocyte cytoskeleton by proteases such as cathepsin L (refs. 8,10). Cathepsin L induction in cultured podocytes is accompanied by an increase in cell motility[10]. This increased motility of *in vitro* podocytes[10,11] is best translated into foot process dynamics *in vivo*, in which podocytes remain locally attached to the GBM, whereas altered foot process dynamics lead to foot process effacement and proteinuria. In some forms of inflammatory glomerular diseases, such as crescentic glomerulonephritis, podocytes can move out of their microenvironment into areas of crescentic glomerular damage[12]. The concept of dynamic podocyte foot processes dates back to the 1970s, when studies showed that infusion of polycations can change foot process dynamics and cause their effacement[13]. Moreover, this event could be reversed by the infusion of polyanions[13]. Even though at present it is not possible to image foot process dynamics continuously in live animals, the results from the above-mentioned studies suggest a highly dynamic podocyte foot process system. Moreover, electron-microscopic analysis commonly reveals small areas of foot process effacement in healthy kidneys possibly representing foot processes during a transitional stage[14]. Cancer cell motility is another situation in which cells can be hyperdynamic or participate in tissue invasion[15]. To explore potential molecular similarities between migrating cancer cells and motile podocytes during proteinuric conditions *in vitro*[10], we decided to study molecules associated

[1]Nephrology Division and Program in Glomerular Disease, Department of Medicine, Massachusetts General Hospital, Harvard Medical School, Boston, Massachusetts 02129, USA. [2]Institute for Anatomy and Cell Biology, Homburg University, Homburg 66421, Germany. [3]The Center for Transgene Technology and Gene Therapy, Flanders Interuniversity Institute for Biotechnology, Katholieke Universiteit Leuven, 3000 Leuven, Belgium. [4]Department of Transgene Technology and Gene Therapy, Vlaams Interuniversitair Instituut voor Biotechnologie, 3000 Leuven, Belgium. [5]Division of Matrix Biology, Department of Medicine, Beth Israel Deaconess Medical Center, Boston, Massachusetts 02215, USA. [6]Division of Nephrology, Department of Internal Medicine, University of Michigan, Ann Arbor, Michigan 48109, USA. [7]Medizinische Poliklinik, University of Munich, Munich 80336, Germany. [8]Renal Immunopathology Laboratory, Associazione Nuova Nefrologia and Fondazione D'Amico per la Ricerca sulle Malattie Renali, c/o San Carlo Borromeo Hospital, Milan, 20153, Italy. [9]Immunology Research Centre, St. Vincent's Hospital, Melbourne, Victoria 3065, Australia. [10]Department of Pathophysiology and Human Molecular Genetics, Centro de Investigaciones Biológicas, Madrid, 28040, Spain. [11]Department of Pathology, Université de Montréal, Montreal, Quebec H3T 1J4, Canada. [12]Department of Medicine, Mount Sinai School of Medicine, New York, New York 10029, USA. Correspondence should be addressed to J.R. (jreiser@partners.org).

Received 5 September; accepted 20 November; published online 16 December 2007; doi:10.1038/nm1696

with cellular motility, such as the urokinase plasminogen activator receptor, uPAR (refs. 16,17), *in vivo* during proteinuric disease.

uPAR is a glycosylphosphatidylinositol (GPI)-anchored protein that has been shown to be a proteinase receptor for urokinase but has also been involved in nonproteolytic pathways, mainly through its ability to form signaling complexes with other transmembrane proteins such as integrins, caveolin and G-protein-coupled receptors[17]. uPAR has important roles in wound healing, inflammation and stem cell mobilization, as well as in severe pathological conditions such as HIV-1 infection, tumor invasion and metastasis[18]. uPAR also exerts its function through interactions with proteins present in the extracellular matrix, including vitronectin[19,20].

Here, we analyzed the role of uPAR in podocytes during normal and disease conditions. We have analyzed mice deficient in *Plaur* (ref. 21), *Plau* (ref. 22), *Vtn* (ref. 23) and *Itgb3* (ref. 24), which encode uPAR, urokinase, vitronectin and β3 integrin respectively, and have challenged them with LPS, a treatment known to cause foot process effacement and proteinuria[9]. We show that uPAR is dispensable for normal renal filtration, yet it is required in podocytes, but not in endothelial cells, for loss of renal permselectivity. We also show that the signal originating from uPAR in podocytes is independent of its major ligand, urokinase, but is sufficient to cause proteinuria through its association with cell-matrix receptors. We propose a mechanism whereby uPAR activates αvβ3 integrin within lipid rafts[25], causing proteinuria. Pharmacologically, this mechanism can be antagonized with small molecule integrin inhibitors or antibodies, leading to potent reduction of urinary protein loss.

RESULTS

uPAR induction in human and rodent proteinuric diseases

uPAR protein is expressed in human glomerular cells (**Fig. 1a**), including podocytes, which are identified by synaptopodin labeling[11]. We performed quantitative RT-PCR with glomeruli isolated from human kidney biopsies (**Fig. 1b**)[26]. We analyzed *PLAUR* expression in RNA samples from individuals without glomerular disease ($n = 8$) and in individuals with focal segmental glomerulosclerosis (FSGS, $n = 14$) and diabetic nephropathy ($n = 20$), both conditions with podocyte foot process effacement and proteinuria[6]. We found low-level glomerular *PLAUR* mRNA expression in individuals without glomerular disease (**Fig. 1b**). In contrast, individuals with biopsy-proven FSGS had a significant increase in glomerular *PLAUR* expression (FSGS 0.35 ± 0.17 versus control 0.14 ± 0.02, $^*P < 0.05$; **Fig. 1b**). An even stronger induction of glomerular *PLAUR* mRNA expression (0.69 ± 0.21 versus control 0.14 ± 0.02, $^*P < 0.012$) was found in people with diabetic nephropathy (**Fig. 1b**).

To test which glomerular cells have increased uPAR expression, we examined the localization of uPAR within the kidney in three different animal models of proteinuria and podocyte foot process effacement, including the puromycin aminonucleoside nephrosis (PAN) model[27], the LPS model of transient proteinuria[9] and the NZB/W F1 model of systemic lupus erythematosus[28]. We found low expression of uPAR in glomeruli from control rats or mice (**Fig. 1c**). uPAR was partially

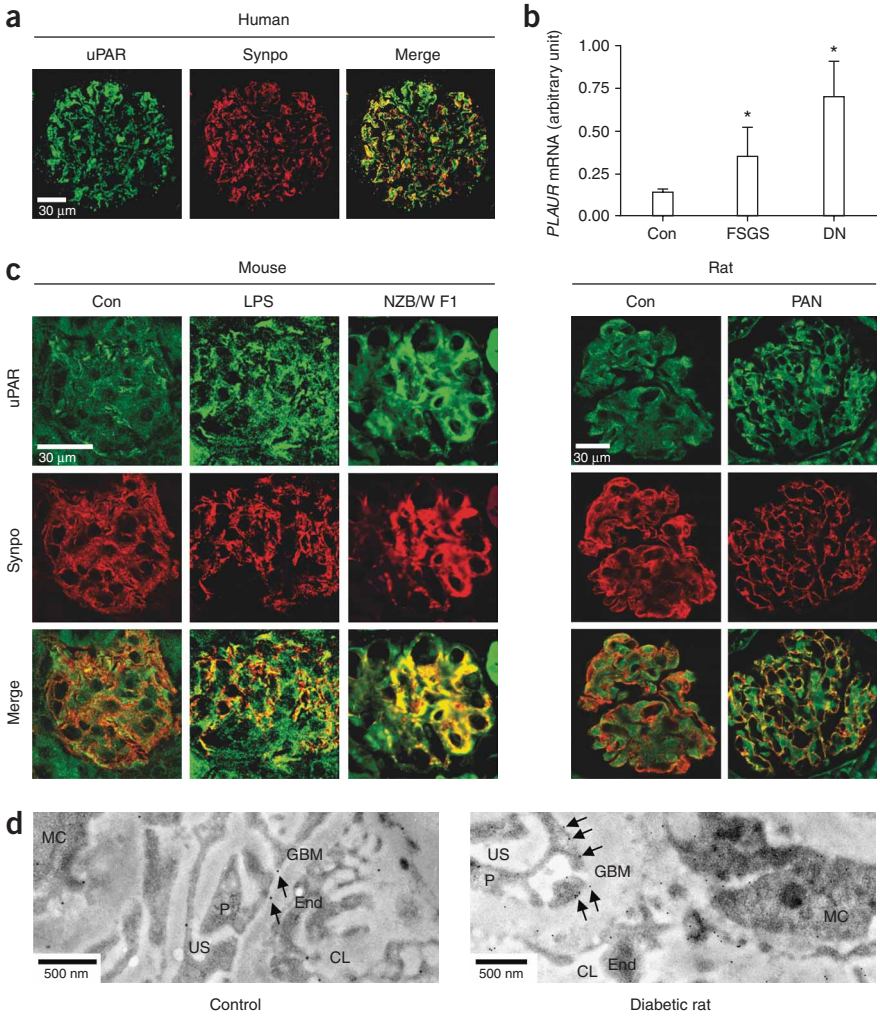

Figure 1 uPAR is induced in podocytes in proteinuric patients and experimental proteinuric models. (**a**) uPAR protein (green) is expressed in glomeruli of human kidney. Some uPAR is found in podocytes, as shown by double immunofluorescence with the podocyte marker synaptopodin (synpo, red) resulting in a partial yellow overlap. (**b**) Induction of glomerular *PLAUR* mRNA in proteinuric subjects. Quantitative real-time RT-PCR was performed on glomeruli isolated from human biopsies. Glomerular *PLAUR* mRNA is upregulated in FSGS ($n = 14$) and diabetic nephropathy (DN, $n = 20$; see also **Supplementary Table 1** online). (**c**) Induction of uPAR protein in podocytes in murine models of proteinuria, as revealed by immunocytochemistry. uPAR expression (green) is low in control glomeruli (Con) from rat or mouse and colocalizes partially with the podocyte marker synaptopodin (Synpo, red). In podocytes from animals with proteinuria (PAN, LPS, NZB/W F1), uPAR expression is substantially induced in podocytes, resulting in a yellow overlap with synaptopodin (Merge). uPAR expression in New Zealand black/white (NZB/W) F1 mice (Lupus) appears more segmental within the glomerulus. (**d**) Immunogold analysis of uPAR in glomerular walls of normal and 12-month-old diabetic rats. uPAR expression is found in all cells of the glomerulus including podocytes. uPAR expression is substantially induced in foot processes of diabetic rats. Black arrows mark uPAR expression in podocyte foot processes. MC, mesangial cell; P, podocyte; End, endothelial cell; US, urinary space; CL, capillary lumen.

Table 1 Quantitative analysis of uPAR expression and localization in glomeruli from normal and diabetic rats

	uPAR morphometric analysis				
	Endothelial luminal membrane	Endothelial basal membrane	Podocyte luminal membrane	Podocyte basal membrane	Mesangial membrane
Normal, 3 months	0.26 ± 0.06[a] (216.01 μm)[b]	0.20 ± 0.05 (213.89 μm)	0.24 ± 0.03 (576.86 μm)	0.19 ± 0.03 (258.95 μm)	0.38 ± 0.05 (196.62 μm)
Normal, 12 months	0.23 ± 0.06 (144.63 μm)	0.18 ± 0.04 (141.51 μm)	0.27 ± 0.05 (288.68 μm)	0.19 ± 0.05 (138.03 μm)	0.30 ± 0.06 (240.94 μm)
Diabetic, 3 months	0.38 ± 0.05[c] (212.17 μm)	0.27 ± 0.06 (210.15 μm)	0.33 ± 0.03 (519.05 μm)	0.29 ± 0.04[c] (267.88 μm)	0.42 ± 0.06 (213.83 μm)
Diabetic, 12 months	0.36 ± 0.09[c] (219.79 μm)	0.37 ± 0.08[c] (234.75 μm)	0.24 ± 0.06 (586.03 μm)	0.27 ± 0.03[c] (256.68 μm)	0.41 ± 0.08 (253.73 μm)
Control for specificity	0.02 ± 0.01 (95.06 μm)	0.05 ± 0.03 (89.29 μm)	0.05 ± 0.04 (133.65 μm)	0.04 ± 0.03 (75.57 μm)	0.07 ± 0.03 (172.70 μm)

[a]Particles per μm of membrane. [b]Total length of membrane measured. [c]Significantly different from corresponding value in normal animals. *$P < 0.005$; $n = 3$ animals for each time point.

localized in podocytes, as indicated by colabeling with synaptopodin, a marker of this cell type[29]. In contrast with the control results, expression of uPAR protein in all proteinuria models was substantially increased in glomerular cells, including podocytes (**Fig. 1c**). Of note, in NZB/W F1 lupus mice, uPAR was preferentially found in crescentic areas of the glomerulus (**Fig. 1c**). Such a distribution has been reported in murine glomerulonephritis, in which podocytes can populate cellular crescents[12]. We also found expression of uPAR in proximal tubular cells that appeared unchanged under normal and disease conditions (data not shown). We next used cultured differentiated podocytes, which express all known podocyte proteins including nephrin and podocin[30] (**Supplementary Fig. 1b**), to study the expression and localization of uPAR. Increased uPAR protein expression was observed in LPS- and PAN-treated cells (**Supplementary Fig. 1c**) in which uPAR was preferentially located at the podocyte cell membrane (**Supplementary Fig. 1d**). Analysis of the uPAR ligand vitronectin revealed prominent staining of vitronectin in human kidney podocytes (**Supplementary Fig. 2a** online). We detected an increase in vitronectin labeling in the podocytes of PAN rats, LPS and lupus mice when compared to controls (**Supplementary Fig. 2b**). Overall, the vitronectin expression profiles in podocytes were similar to the pattern we have observed for uPAR.

To define the subcellular localization of uPAR within glomerular cells, including within podocytes, we analyzed uPAR localization in normal and diabetic rats (**Fig. 1d**), as *PLAUR* mRNA induction is strongest during diabetic nephropathy in humans (**Fig. 1b**). We performed semiquantitative immunogold analysis of uPAR in glomerular walls of normal and 3- and 12-month-old diabetic rats[31]. Under normal conditions, uPAR expression was observed in all cell types of the glomerulus (**Table 1**), including podocytes (**Fig. 1d**). The morphometric analysis revealed a homogeneous distribution of uPAR in podocytes, mesangial and endothelial cells (**Table 1**). Twelve-month-old diabetic rats showed increased uPAR labeling in all cells of the glomerular tuft (**Fig. 1d**). Notably, podocyte uPAR expression was increased in 3- and 12-month-old diabetic rats, but only in basal membrane aspects of the foot processes.

uPAR in podocytes is required for effacement and proteinuria

To explore whether uPAR has a direct role in regulating podocyte foot process structure and function, we next compared the foot process morphology of wild-type and *Plaur*$^{-/-}$ mice before and after administration of LPS. Morphologically, there was no difference between wild-type and *Plaur*$^{-/-}$ mice in podocyte foot process structure (**Fig. 2a**). However, after LPS injection, we found podocyte foot process effacement in wild-type but not *Plaur*$^{-/-}$ mice (**Fig. 2a**), suggesting a functional link between the development of podocyte foot process effacement and uPAR expression. To test whether the protection from LPS-induced foot process effacement in *Plaur*$^{-/-}$ mice could be overcome by restoring glomerular uPAR expression, we used our previously reported gene delivery protocol to deliver *Plaur* cDNA[8,32]. Twenty-four hours after gene delivery of a plasmid encoding uPAR, we found uPAR expression in glomerular cells, including podocytes, of *Plaur*$^{-/-}$ mice (**Fig. 2b**). To monitor expression of uPAR after gene delivery, we performed immunoblotting. Fourteen hours after *Plaur* delivery, we found uPAR protein in the liver and, at lower expression levels, in glomeruli (**Fig. 2c**). The restoration of uPAR expression did not change the morphology of podocyte foot processes (**Fig. 2d**), suggesting that exogenous uPAR behaves similarly to endogenous uPAR. However, concomitant administration of LPS and *Plaur* cDNA to *Plaur*$^{-/-}$ mice resulted in foot process effacement (**Fig. 2d**), similarly to the results in LPS-treated wild-type mice expressing endogenous uPAR (**Fig. 2a**). In contrast, we did not find any foot process changes in *Plaur*$^{-/-}$ mice that had received vector control, even after coadministration of LPS (**Fig. 2d**).

To study the functional consequences of uPAR reconstitution, we analyzed the urinary protein excretion of wild-type, *Plaur*$^{-/-}$ and uPAR-reconstituted *Plaur*$^{-/-}$ mice before and after LPS injection. Whereas PBS-treated control mice and *Plaur*$^{-/-}$ mice did not have any significant proteinuria, the injection of LPS induced significant proteinuria in wild-type but not *Plaur*$^{-/-}$ mice and *Plaur*$^{-/-}$ mice that had received control plasmids (**Fig. 2e**). These data indicate that *Plaur*$^{-/-}$ mice are protected from urinary protein loss. Most notably, *Plaur*$^{-/-}$ mice reconstituted with *Plaur* cDNA developed heavy proteinuria but, like wild-type mice, only after LPS injection

(**Fig. 2e**). The degree of proteinuria was comparable in LPS-treated wild-type and *Plaur* cDNA–reconstituted *Plaur*$^{-/-}$ mice. In summary, these data strongly suggest that uPAR is required for the development of LPS-induced proteinuria in mice.

To test whether uPAR exerts its effects on proteinuria development solely by altering podocyte function or whether it also alters glomerular endothelial cell function, we carried out gene transfer of *Plaur* cDNA under the control of two different promoters allowing cell-specific expression of uPAR in podocytes (*NPHS2-Plaur*)[33] or endothelial cells (*ICAM2-Plaur*)[34]. Cell type–specific expression of uPAR was monitored by double immunofluorescence labeling of uPAR and synaptopodin (**Fig. 2f**) or the endothelial marker CD31 (ref. 35; **Fig. 2g**). Whereas the expression of uPAR in podocytes was required for LPS-induced proteinuria, the expression of uPAR in endothelial cells was associated with LPS resistance (**Fig. 2h**). These results show that podocyte but not endothelial uPAR is required and sufficient for LPS-induced proteinuria.

uPAR orchestrates podocyte motility

To better understand uPAR function in podocytes, we considered uPAR's role in cell motility[17]. Podocyte foot process effacement may represent a motile event, resulting in spreading of podocyte foot processes on the GBM. Thus, we studied podocyte motility before and after stable knockdown of *Plaur* with siRNA (**Supplementary Fig. 3a**,**b** online). We then used a modified multiwell Boyden chamber assay to assess the random migration of differentiated podocytes on type 1 collagen (data not shown) and vitronectin, a known binding partner of uPAR (refs. 19,20) that is induced in proteinuric glomeruli (**Supplementary Fig. 2b**). LPS or PAN treatment for 24 h significantly promoted the migration of wild-type podocytes (**Fig. 3a**,**b**). In contrast, the knockdown of *Plaur* significantly decreased the number of migrating podocytes under normal conditions and after treatment with LPS or PAN (**Fig. 3a**,**b**). These results show that podocyte motility is increased in response to LPS or PAN in a uPAR-dependent manner.

We also analyzed the effect of uPAR on the spatial motility of podocytes with a modified scrape-wound assay[11]. Compared to control cells, LPS or PAN treatment significantly promoted podocyte wound closure after 24 h (**Fig. 3c**,**d**), a finding that we also obtained in a similar pattern at time points 12, 24 and 48 h (**Supplementary Fig. 3c**). The addition of external urokinase did not alter podocyte directional migration (**Supplementary Fig. 3d**), but knockdown of *Plaur* strongly reduced podocyte-directed motility before and after administration of LPS or PAN (**Fig. 3c**,**d** and **Supplementary**

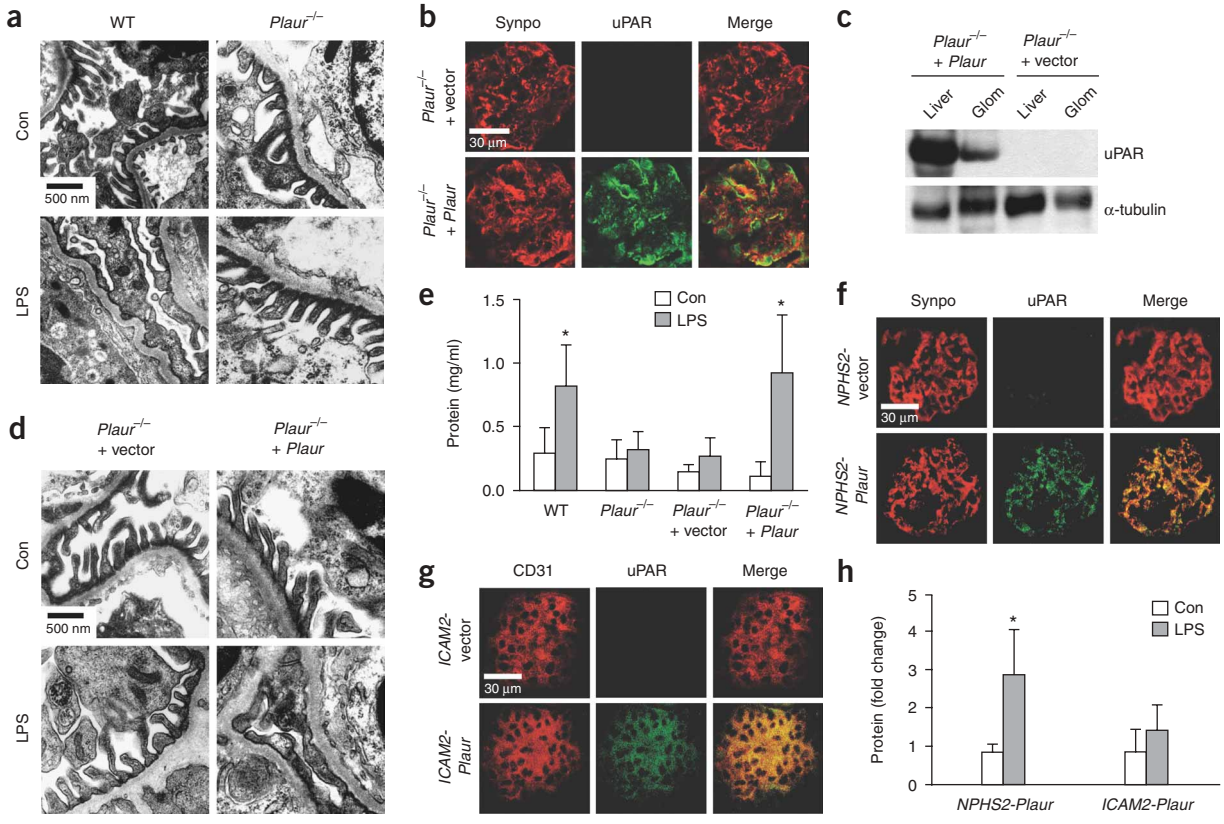

Figure 2 uPAR is required in podocytes for the development of foot process effacement and proteinuria. (**a**) LPS treatment leads to foot process effacement in wild-type but not *Plaur*$^{-/-}$ mice. (**b**) Restoration of *Plaur* expression in *Plaur*$^{-/-}$ mice by transient gene transfer leads to podocyte uPAR expression. (**c**) Immunoblot showing exogenous uPAR expressed in liver and glomeruli from *Plaur*$^{-/-}$ mice 14 h after gene delivery. (**d**) Gene delivery of *Plaur* cDNA or empty vector does not change the ultrastructure of podocyte foot processes in *Plaur* $^{-/-}$ mice. However, concomitant LPS treatment leads to foot process effacement in *Plaur*-restored *Plaur*$^{-/-}$ mice. (**e**) Urine Bradford assay. The injection of LPS induces significant proteinuria in wild-type mice but not in *Plaur*$^{-/-}$ mice or *Plau*$^{-/-}$ mice that received control plasmids. *Plaur*$^{-/-}$ mice reconstituted with *Plaur* cDNA develop proteinuria, but only after LPS injection. (**f**) Podocyte uPAR expression in *Plaur*$^{-/-}$ mice after gene transfer of *NPHS2*-driven *Plaur* cDNA (*NPHS2-Plaur*). (**g**) Endothelial uPAR expression in *Plaur*$^{-/-}$ mice after gene transfer of *ICAM2*-driven *Plaur* cDNA (*ICAM2-Plaur*). (**h**) Fold change in urinary protein loss in *Plaur*$^{-/-}$ mice after gene transfer of *NPHS2-Plaur* or *ICAM2-Plaur* with or without LPS treatment. (See also **Supplementary Table 1**.)

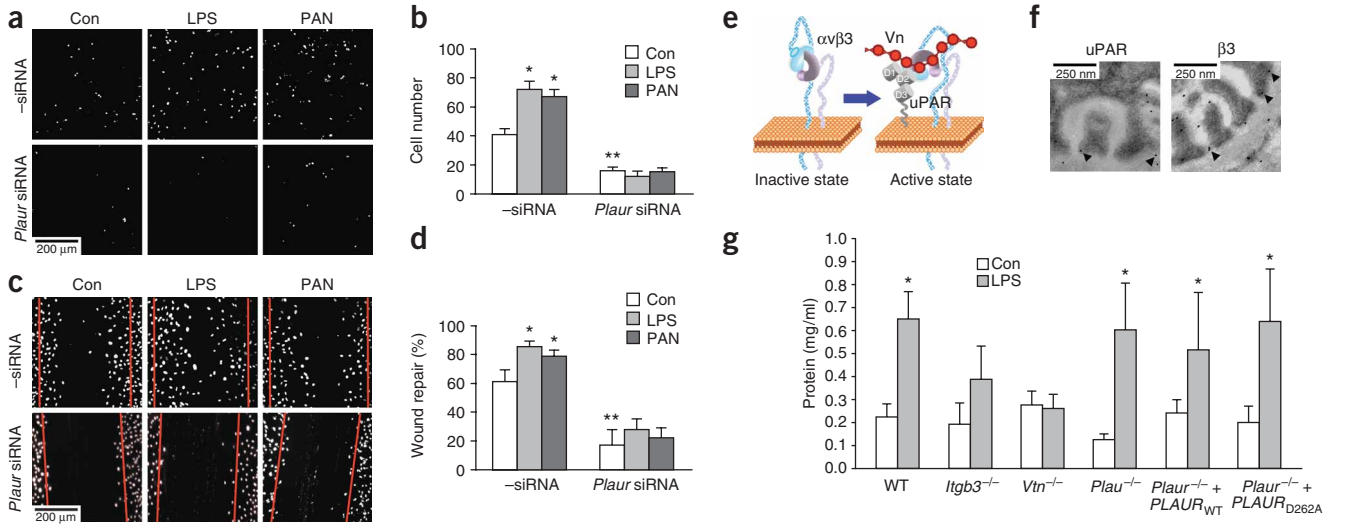

Figure 3 uPAR-mediated podocyte motility and proteinuria involves αvβ3 integrin and vitronectin. (**a**) Boyden chamber assay of podocytes grown on vitronectin. (**b**) LPS and PAN treatment for 24 h promoted podocyte migration. Knockdown of *Plaur* by siRNA strongly reduced podocyte migration. (**c**) Directed podocyte motility assay. 24 h after scraping of the podocyte cell layer, WT cells have started to migrate into the wound track. Treatment with LPS or with PAN significantly enhanced directed podocyte motility. (**d**) *Plaur* siRNA–expressing podocytes showed defects in directed motility, as reflected by fewer cells having migrated into the wound track. Scale bar, 200 μm. (**e**) Schematic depiction of uPAR in complex with αvβ3 integrin and vitronectin. (**f**) Immunogold analysis of uPAR and β3 integrin in podocyte foot processes. Both uPAR and β3 integrin are often found close to the slit diaphragm (black arrowheads). (**g**) The absence of *Plaur* (see **Fig. 2e**), *Itgb3* and *Vtn* is associated with lack of proteinuria before and after LPS. In contrast, $Plau^{-/-}$ mice have no proteinuria under normal conditions but readily develop proteinuria after LPS. The same is observed in LPS-treated $Plaur^{-/-}$ mice after gene delivery of *PLAUR* cDNA ($PLAUR_{WT}$) or *PLAUR* cDNA encoding a uPAR that is deficient in binding of α3β1 integrin ($PLAUR_{D262A}$). (See also **Supplementary Table 1**.)

Fig. 3c). Together, these data show that uPAR is important for podocyte motility.

uPAR activates αvβ3 integrin in podocytes

Because uPAR is a GPI-anchored protein without a cytoplasmic tail, it is generally believed that signal transduction from uPAR involves lateral interactions with membrane proteins such as integrins[17]. Most recently, one study showed that uPAR-induced cell adhesion and migration requires vitronectin binding, which can occur independently of uPAR interactions with integrins[20]. Podocyte motility on vitronectin is enhanced in a uPAR-dependent fashion (**Fig. 3a–d**), and vitronectin is induced in glomeruli during proteinuria (**Supplementary Fig. 2b**). Thus, it appeared possible that a uPAR-vitronectin complex or an uPAR-vitronectin-integrin complex facilitates podocyte motility and promotes foot process effacement in response to LPS. Integrins can be in an inactive or active conformation (ref. 36; **Fig. 3e**). The latter conformation is stimulated by integrin association with interacting agonists, such as domain 3 of uPAR, which is important for α5β1 integrin interaction[37,38]. An integrin-interacting sequence in domain 2 of uPAR, which acts as a chemotactic epitope activating αvβ3-dependent signaling pathways, has recently been identified[39]. Given our findings of uPAR and vitronectin expression in the glomerulus, we were particularly interested in the vitronectin receptor αvβ3 integrin[36]. Indeed, the localization of αvβ3 integrin[32] and the distribution of uPAR (**Fig. 3f**) in podocyte foot processes were similar. In addition, uPAR interacts with β3 integrin (**Supplementary Fig. 4a** online). Thus, we hypothesized that αvβ3 integrin may provide a functional link between uPAR, podocyte migration and development of proteinuria. Mice lacking β3 integrin or the αvβ3 integrin ligand vitronectin are protected from LPS-induced proteinuria (**Fig. 3g**). This means that both vitronectin and β3 integrin are required for LPS-induced proteinuria, but either one is dispensable for normal renal development and function (**Fig. 3g** and data not shown). Given the extent of the published uPAR interactome and the importance of α3β1 integrin in podocyte development[3], we also analyzed the potential contribution of α3β1 integrin to the uPAR signaling cascade in podocytes by using a cDNA for *PLAUR* that encodes the uPAR mutant D262A, which is unable to bind α3β1 integrin in humans[38] and in mice (**Supplementary Fig. 4b**). The expression of $uPAR_{D262A}$ in podocytes led to the development of LPS-induced proteinuria (**Fig. 3g**), supporting the idea that uPAR in podocytes preferentially signals through αvβ3 integrin. Because uPAR is involved in pathways both dependent on and independent of urokinase[17], we also explored the contribution of urokinase to uPAR-dependent proteinuria pathways by treating $Plau^{-/-}$ mice with LPS. Notably, these mice developed proteinuria, suggesting that urokinase is not required for the LPS-mediated effects of uPAR on the kidney filtration barrier (**Fig. 3g**).

$Plaur^{-/-}$, $Itgb3^{-/-}$ and $Vtn^{-/-}$ mice have no overt renal phenotypes under normal conditions (**Figs. 2e** and **3g**), suggesting that uPAR signaling in podocytes is not required for normal glomerular filtration. However, all of these molecules are required for the development of urinary protein loss. In light of these findings, we reasoned that changes in the activation of αvβ3 integrin under disease conditions may cause increased podocyte motility and foot process effacement after administration of LPS. To explore this idea, we studied the expression of total and active β3 integrin in kidney sections from wild-type and $Plaur^{-/-}$ mice. We visualized total podocyte β3 integrin expression in wild-type and $Plaur^{-/-}$ mice before and after injection of LPS (**Fig. 4a**). The expression of β3 integrin in podocytes was unchanged in wild-type and $Plaur^{-/-}$ mice both before and after LPS administration (**Fig. 4a**). We next looked for the presence of active β3

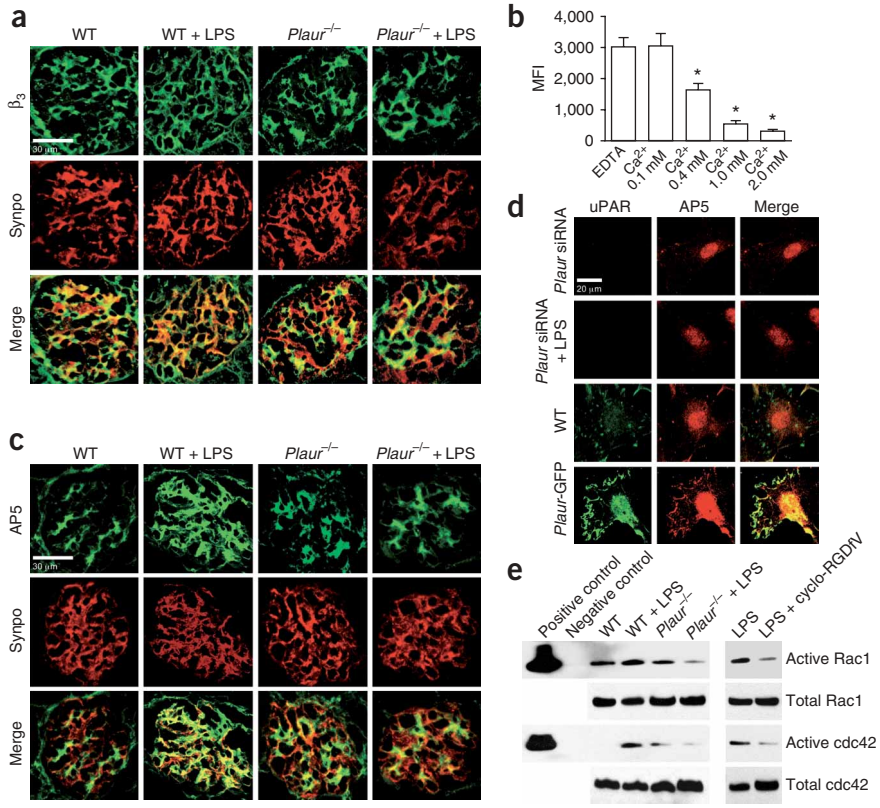

Figure 4 uPAR activates β3 integrin. (**a**) Double immunofluorescence staining for β3 integrin (green) and the podocyte marker synaptopodin (red) in glomeruli from WT and *Plaur*$^{-/-}$ mice before and after treatment with LPS, as evaluated by confocal microscopy. LPS treatment does not change podocyte β3 integrin in WT and *Plaur*$^{-/-}$ mice. (**b**) Flow cytometry for AP5 antibody binding to LPS-treated podocytes in the presence of various amounts of Ca^{2+}. (**c**) Same as in **a**, but now in the presence of the antibody AP5. LPS treatment induces staining for AP5 in WT but not *Plaur*$^{-/-}$ mice. (**d**) Immunofluorescence analysis and confocal microscopy of AP5 labeling (red) and uPAR staining (green) in *Plaur* siRNA–treated podocytes before and after LPS treatment, in control podocytes and in podocytes overexpressing GFP-*Plaur*. (**e**) Activity assay of the small GTPases cdc42 and Rac1 in isolated glomeruli from WT and *Plaur*$^{-/-}$ mice before and after treatment with LPS. In some experiments, WT mice were treated with LPS and cyclo-RGDfV, which blocks αvβ3 integrin. (See also **Supplementary Table 1**.)

integrin in podocytes, for which we used AP5 antibody. This antibody recognizes an N-terminal epitope of β3 integrin that is only accessible when the integrin is in its active conformation[40]. To evaluate whether AP5 could be used to detect active β3 integrin in podocytes, we first tested the effect of divalent cations on the binding pattern of AP5 to β3 integrin by flow cytometry of normal (data not shown) and LPS-treated cultured podocytes[41] (**Fig. 4b**). We found a calcium-dependent binding pattern of AP5 to β3 integrin similar to that previously reported in other cell types[41]. Active β3 integrin abundance was low in wild-type (**Fig. 4c**, WT) and *Plaur*$^{-/-}$ mice (**Fig. 4c**, *Plaur*$^{-/-}$) under normal conditions. This finding suggests that αvβ3 integrin has a low basal activity even in the absence of uPAR. LPS treatment of wild-type mice was associated with a strong induction of podocyte AP5 labeling (**Fig. 4c**). This induction was absent in LPS-treated *Plaur*$^{-/-}$ mice (**Fig. 4c**, *Plaur*$^{-/-}$ + LPS). We also observed colocalization of AP5 labeling at sites of uPAR overexpression in cultured podocytes, but not in podocytes in which *Plaur* was downregulated by siRNA treatment (**Fig. 4d**), suggesting that uPAR is required for the activation of β3 integrin in podocytes.

As an additional readout for active β3 integrin expression, we analyzed the activity of the small GTPases Cdc42 and Rac1 in glomerular lysates from wild-type and *Plaur*$^{-/-}$ mice before and after administration of LPS (**Fig. 4e**)[42]. The activity of Rac1 was increased in LPS-treated wild-type but not *Plaur*$^{-/-}$ mice (**Fig. 4e**, top). We observed a similar induction pattern for Cdc42 activity (**Fig. 4e**, bottom). In some experiments, we co-injected wild-type mice with LPS and cyclo-[Arg-Gly-Asp-D-Phe-Val]-RGDfV (cyclo-RGDfV), known from clinical cancer trials as Cilengitide), which is used as a specific inhibitor of αvβ3 integrin[43]. This treatment inhibited the induction of active Rac1 and Cdc42 in the glomeruli of LPS-treated mice (**Fig. 4e**). These findings support the concept that uPAR is required for the activation of podocyte αvβ3 integrin after LPS treatment.

We next looked for subcellular compartments in which uPAR and β3 integrin can associate with each other. Studies suggest that many regions of the podocyte foot process membrane and slit diaphragm are rich in cholesterol, and several slit diaphragm proteins, such as podocin and nephrin, are associated with lipid rafts[44]. Plasma membrane lipid rafts help to compartmentalize signal transduction events within different membrane regions[25], and uPAR, as a GPI-anchored protein, is known to be found in lipid-rich membrane compartments[17]. We wondered whether uPAR and β3 integrin associate together within lipid rafts in podocytes, and thus we performed sucrose density gradient assays of whole cellular extracts from cultured podocytes before and after LPS treatment (**Fig. 5a**). We found that uPAR and β3 integrin are mainly associated with nonraft fractions in control podocytes. However, after LPS treatment, both uPAR and β3 integrin were enriched within the lipid raft fraction (**Fig. 5a**). The functional association of uPAR and β3 integrin within lipid rafts was fostered by the observation that disruption of lipid rafts by methyl-β-cyclodextrin treatment[45] abrogated the activation of β3 integrin in response to LPS (**Fig. 5b**). These data suggest that β3 integrin can be activated by uPAR within lipid-rich domains of the podocyte plasma membrane.

Interference with αvβ3 integrin modifies proteinuria

If the activation of αvβ3 integrin is a key signal that mediates uPAR-induced cellular events leading to proteinuria, expression of a constitutively active β3 integrin should be sufficient to induce proteinuria, even in the absence of uPAR. Therefore, we used an *ITGB3* cDNA that encodes a protein lacking amino acids 616–690 of the C-terminal region of the β3 ectodomain ($ITGB_{\Delta 616–690}$). This mutation confers constitutive activity to the β3 protein[46]. We performed gene transfer of this active *ITGB3* construct into *Plaur*$^{-/-}$ mice and monitored the activity of β3 integrin in podocytes by immunofluorescent double-labeling of synaptopodin and β3 integrin. We labeled β3 integrin with WOW-1 antibody, which is known to recognize constitutively active β3 protein[47]. *Plaur*$^{-/-}$ mice positive for WOW-1 labeling in podocytes

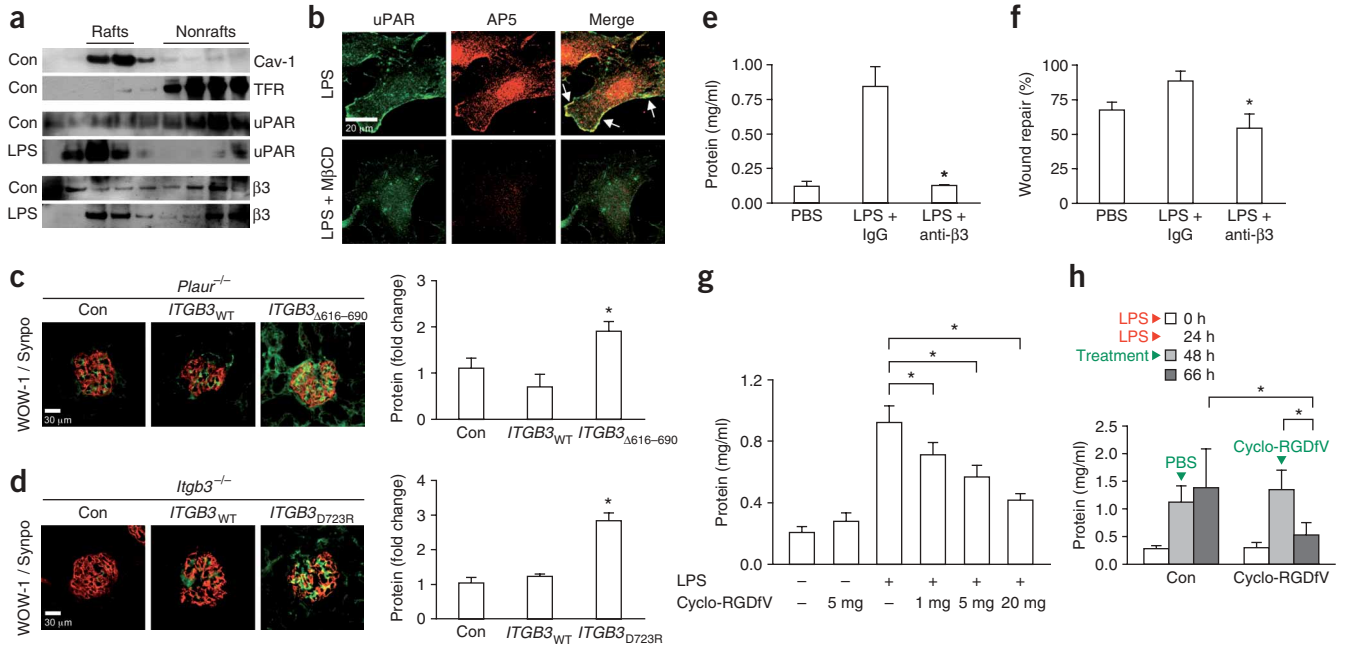

Figure 5 The active uPAR-αvβ3 integrin complex is lipid dependent and its blockade modifies proteinuria. (**a**) Lipid raft assays in cultured podocytes. Cav-1, caveolin-1. The transferrin receptor (TFR) is a nonraft protein control. (**b**) Localization of uPAR and AP5 labeling in podocytes. (**c**) Immunofluorescence of active β3 integrin in glomeruli of *Plaur*$^{-/-}$ mice (Con) or *Plaur*$^{-/-}$ mice that had received β3 integrin cDNA (*ITGB3*$_{WT}$) or β3 integrin 616–690 cDNA (*ITGB3*$_{Δ616–690}$). Corresponding WOW-1 Fab antibody labeling is shown on the left. Gene transfer of *ITGB3*$_{Δ616–690}$ but not of *ITGB3*$_{WT}$ is sufficient to cause proteinuria in *Plaur*$^{-/-}$ mice, even in the absence of LPS. (**d**) Immunofluorescence of active β3 integrin in glomeruli of *Itgb3*$^{-/-}$ (Con) or *Itgb3*$^{-/-}$ mice that had received *ITGB3*$_{WT}$ cDNA or a cDNA encoding the β3 integrin point mutant D723R (*ITGB3*$_{D723R}$). Corresponding WOW-1 Fab antibody labeling is shown on the left. Gene transfer of *ITGB3*$_{D723R}$ but not of *ITGB3*$_{WT}$ is sufficient to cause proteinuria in *Itgb3*$^{-/-}$ mice, even in the absence of LPS. (**e**) Coinjection of LPS and a β3 integrin-blocking antibody (anti-β3) into WT mice prevents proteinuria. (**f**) Coadministration of LPS and antibody to β3 integrin to cultured podocytes reduces podocyte motility. (**g**) Injection of cyclo-RGDfV blocks αvβ3 integrin activity and development of proteinuria in LPS-treated mice in a dose-dependent manner. (**h**) Cyclo-RGDfV treatment of proteinuric mice significantly reduced urinary protein loss at 66 h when compared to proteinuria levels of these mice at 48 h. Control mice were still strongly proteinuric 66 h after the first LPS administration compared to mice that had been injected with cyclo-RGDfV at timepoint 48 h. (See also **Supplementary Table 1**.)

developed proteinuria (**Fig. 5c**), whereas littermates that received normal *ITGB3* or vector control had very low podocyte WOW-1 labeling and no proteinuric response (**Fig. 5c**). We also performed experiments in *Itgb3*$^{-/-}$ mice, but instead of using *ITGB3*$_{Δ616–690}$, we administered *ITGB*$_{D723R}$, which confers constitutive activity as well[48]. The expression of this active β3 integrin mutant was detected by positive WOW-1 labeling in the podocyte and by the induction of heavy proteinuria in *Itgb3*$^{-/-}$ mice (**Fig. 5d**). In contrast with these results, the expression of *Plaur* cDNA (data not shown) or of wild-type *ITGB3* (**Fig. 5d**) in *Itgb3*$^{-/-}$ mice did not result in WOW-1 labeling or urinary protein loss. These data corroborate our findings that activation of β3 integrin is sufficient to cause proteinuria.

We also performed experiments with an antibody that inhibits β3 integrin function. Wild-type mice that were co-injected with LPS and a monoclonal antibody to β3 integrin did not develop proteinuria in response to LPS (**Fig. 5e**). This blocking antibody was also able to reduce podocyte motility significantly during LPS treatment *in vitro* (**Fig. 5f**), connecting increased podocyte motility *in vitro* to the development of proteinuria *in vivo*.

Finally, we used different concentrations of cyclo-RGDfV to specifically block active αvβ3 integrin. Cyclo-RGDfV was injected into LPS-treated wild-type mice (**Fig. 5g**). Whereas the administration of cyclo-RGDfV to normal mice had no effect, mice that received both LPS and cyclo-RGDfV showed an attenuated course of proteinuria in a cyclo-RGDfV dose–dependent manner compared to control mice that had received only LPS (**Fig. 5g**). We also performed a treatment study in which wild-type mice were injected twice with LPS to induce and maintain high levels of proteinuria before some mice received cyclo-RGDfV and control animals received PBS (**Fig. 5h**). We observed a substantial reduction of proteinuria in cyclo-RGDfV–treated mice 18 h after administration of this compound. Proteinuric mice that had received PBS instead did not show any resolution of urinary protein loss during this time (**Fig. 5h**).

These data show that increased activity of αvβ3 integrin is important for proteinuria development and demonstrates the feasibility of treating proteinuria by pharmacologically interfering with αvβ3 integrin in podocytes.

DISCUSSION

Proteinuria is a predictor of poorer outcome and faster progression of renal insufficiency[1]. In an attempt to slow down progression of renal disease, the mainstay of therapy is blockade of the renin-angiotensin system[49]. Other treatments, including immunomodulators such as steroids, cyclosporine and alkylating agents, depend on the clinical and histopathological diagnosis. Therapeutic intervention for proteinuric kidney diseases is hampered by at least two key points: interventions are only aimed to slow down the progression of glomerular disease, and cell-specific therapies for proteinuria syndromes are presently not available. Here we describe a mechanism in podocytes that can be targeted pharmacologically. We found an induction of uPAR expression in podocytes during proteinuric kidney diseases

(**Fig. 1b**). uPAR is required for podocyte migration and LPS-induced foot process effacement and proteinuria in mice through a mechanism that includes lipid-dependent activation of αvβ3 integrin. Collectively, our findings define a new signaling pathway in podocytes that involves uPAR, αvβ3 integrin and vitronectin. uPAR is expressed in all glomerular cells, yet it is not required for normal renal function, as the *Plaur*$^{-/-}$ mice have a normal renal phenotype. Of note, uPAR is required for the development of podocyte foot process effacement and proteinuria, which suggests that uPAR-inducible pathways are required for the remodeling of the filtration barrier. uPAR's importance in the development of proteinuria stems from its action in podocytes, which we showed by using cell-specific promoter elements. Nonetheless, the role of uPAR in the other glomerular cell types, as well as the potential interactions podocyte uPAR may have with other integrins and nonintegrins, needs to be studied further.

We recently described LPS resistance in mice lacking cathepsin L (ref. 8) and B7-1 (ref. 9) similar to our data with mice lacking uPAR. Notably, there is data linking Ras signaling with the urokinase system and with cathepsin L in cancer cells[50], and B7-1 in podocytes is stimulated by LPS, as are cathepsin L (ref. 8) and uPAR. It will be necessary to see how all these pathways cooperate. The functional value of active αvβ3 integrin as a downstream effector for increased podocyte motility, which in this case equals foot process effacement and proteinuria, is an attractive outlook for integrin or uPAR inhibitor studies in humans. Because blockade of uPAR and αvβ3 integrin are possible interventions that are currently being studied in clinical cancer trials (such as the trial of Cilengitide in glioblastoma patients), these approaches may prove to have additional benefits as cell-specific treatments of urinary protein loss.

METHODS

Antibodies. Antibodies used in this study are listed with their sources as follows: AP5 antibody to active β3 integrin, Genetic Testing Institute; antibody to WOW-1 fragment (Fab)[47] was a gift (see Acknowledgments); monoclonal antibody to CD61, BD Pharmingen; antibodies to CD31 (ER-MP12), vitronectin (H-270) and uPAR (FL-290), Santa Cruz Biotechnology; polyclonal antibody to uPAR-1, R&D Systems; monoclonal antibody to α-tubulin, Calbiochem; polyclonal antibody to β3 integrin, Chemicon; polyclonal antibody to caveolin-1 and monoclonal antibodies to glyceraldehyde 3-phosphate dehydrogenase (GAPDH), Flag epitope, hemagglutinin and the transferrin receptor, Sigma; mouse monoclonal antibody to synaptopodin (G1), rabbit polyclonal antibody to synaptopodin (NT; ref. 29) and rabbit polyclonal antibody to podocin (ref. 44) were described before; rabbit polyclonal antibody to nephrin was also a gift (see Acknowledgments).

Animals and treatments. All animal studies were approved by the Subcommittee on Research Animal Care of the Massachusetts General Hospital, protocol number 2004N000289/2. All mice were on either a C57BL/6 background or a mixed background of 75% C57BL/6 and 25% 129 Swiss. *Plaur*$^{-/-}$ mice[21], *Plau*$^{-/-}$ mice[22], *Vtn*$^{-/-}$ mice[23] and *Itgb3*$^{-/-}$ mice[24] were described before. We used the LPS mouse and rat PAN models as previously reported[9,27]. NZB/W F1 mice were purchased from the Jackson Laboratory at 19 weeks of age and analyzed after 20 weeks, when proteinuria and lupus glomerulonephritis were present. For the diabetic nephropathy rat model, we used Sprague-Dawley rats treated with streptozotocin[30].

Human subjects. Human renal biopsies were obtained with informed consent and were collected in a multicenter study (the European Renal cDNA Bank) according to the guidelines of the European Renal cDNA Bank Consortium. We analyzed microdissected glomeruli from 34 individuals with proteinuric diseases (FSGS; $n = 14$; diabetic nephropathy, $n = 20$) and 8 control subjects. Control tissue was derived from pretransplantation kidney biopsies during cold ischemia time from seven living and one cadaveric donor ($n = 8$).

Quantitative real-time PCR. We performed TaqMan real-time RT-PCR as previously described[26].

Immunocytochemistry. We stained human glomerular biopsies with uPAR-, vitronectin- or synaptopodin-specific antibodies following standard protocols[8]. We immunolabeled cultured podocytes as previously described[8,9].

Transmission electron microscopy, immunoelectron microscopy and morphometry. We performed transmission electron microscopy and immunoelectron microscopy according to the standard protocols[8,9]. We recorded micrographs of immunolabeled renal glomeruli (>20 micrographs per animal and time point) and evaluated them using morphometrical techniques[51].

GTPase activity assay. We measured GTPase activity in glomerular lysates with a Rho/Rac/Cdc42 activation assay kit (Cell Biolabs) following the manufacturer's protocol. We isolated glomeruli from wild-type and *Plaur*$^{-/-}$ mice, some of them treated with LPS ($t = 0$), with cyclo-RGDfV every 8 h for 24 h, or both, by a standard sieve technique[8].

***In vivo* gene delivery.** We performed gene delivery with the TransIT *in vivo* gene delivery system (Mirus) as described previously[8]. We used the following cDNAs and vectors: *PLAUR*, *PLAUR*$_{D262A}$ (ref. 37; see Acknowledgments), wild-type *ITGB3* and the constitutively active form *ITGB3*$_{\Delta 616–690}$ (ref. 45), *ITGB3*$_{D723R}$ (ref. 47), *NPHS2* promoter vector p2.5 (ref. 33; see Acknowledgments) for *NPHS2-Plaur* and *ICAM2* promoter vector[34] for *ICAM2-Plaur*.

Flow cytometry. We exposed differentiated podocytes to LPS before we incubated them with the following calcium solutions in the presence of 5 μg/ml AP5 for 1 h: 1 mM EDTA, PBS without Ca^{2+} or Mg^{2+}, 0.1 mM $CaCl_2$, 0.4 mM $CaCl_2$, 1 mM $CaCl_2$ and 2 mM $CaCl_2$.

Cell culture and transient transfection. We transfected HEK293 cells and podocytes as reported previously[11].

Western blotting and co-immunoprecipitation. We performed immunoblotting and co-immunoprecipitation experiments as described[11].

Migration assay. We analyzed podocyte migration in a 12-well chemotaxis chamber (Neuro Probe) according to the manufacturer's protocol. We studied the directional movement of podocytes with a wound healing assay[11].

Sucrose gradient ultracentrifugation. We performed sucrose gradient ultracentrifugation as described[45].

Blockade of αvβ3 integrin in mice. We injected cyclo-RGDfV (Biomol) at 1, 5 and 20 mg per kg body weight intravenously into mice three times at 8-h intervals. Control mice received an equal amount of PBS instead or a control peptide, cyclo-RAD (Biomol; data not shown). Immediately after the first injection, we injected 200 μg of LPS intraperitoneally into each mouse to induce proteinuria. We collected urine for a Bradford assay 24 h after LPS injection[8].

For cyclo-RGDfV treatment, we injected C57BL/6 mice twice with LPS (at 0 and 24 h) to induce and maintain proteinuria. Forty-eight hours after the first injection, we administered cyclo-RGDfV ($n = 6$) intravenously (25 mg/kg body weight in 0.5 ml of PBS). Controls ($n = 5$) received the same volume of PBS alone. We collected urine at 0, 48 and 66 h for urine protein analysis.

For blockade of β3 integrin with antibody to CD61, we injected wild-type mice with PBS alone (control), LPS and CD61 monoclonal antibody or LPS and IgG isotype control antibody. We administered the antibody intravenously 4 h after LPS injection to a final concentration of 10 μg/ml. We collected urine at time points 0, 4 and 24 h for protein analysis.

Statistical analysis. We performed statistical analyses by the Student's paired or non-paired *t*-test or Mann-Whitney *U*-test. We rejected the null hypothesis at *P* value 0.05. Values are presented as mean ± s.d. unless stated otherwise.

Note: Supplementary information is available on the Nature Medicine website.

ACKNOWLEDGMENTS

Antibody to WOW-1 fragment (Fab) was a gift from S. Shattil (University of California, San Diego, La Jolla, California). Rabbit polyclonal antibody and *NPHS2* promoter vector p2.5 cDNA were gifts from L. Holzman (University of

Michigan). *Vtn*$^{-/-}$ mice were a gift from D. Ginsburg (University of Michigan) and *Itgb3*$^{-/-}$ mice were obtained from R. Kalluri (Beth Israel Deaconess Medical Center, Harvard Medical School, Boston). *PLAUR*$_{D262A\ 37}$ cDNA was a gift from Y. Wei and H.A. Chapman (University of California, San Francisco). J.R. was supported by the KMD Foundation and the Kidney-Urology Foundation of America–American Society of Nephrology (KUFA-ASN) Research. This work was supported by US National Institutes of Health (NIH) grants DK073495 (to J.R.), DK057683, DK062472 and the George M. O'Brien Kidney Center DK064236 (to P.M.). C.W. is the Halpin Scholar of the American Society of Nephrology. C.C.M. was supported by a scholarship of the German Academic Exchange Service. M.M.A. was supported by NIH training grant T32DK007540. Gene expression studies of uPAR in human disease were performed in the framework of the European renal cDNA bank. We thank all members of the European Renal cDNA Bank and their patients for their support (for participating centers at the time of the study, see ref. 26). Part of the electron microscopy work was performed in the Microscopy Core facility of the Massachusetts General Hospital Program in Membrane Biology and was supported by an NIH Program Project grant (DK38452).

Published online at http://www.nature.com/naturemedicine
Reprints and permissions information is available online at http://npg.nature.com/reprintsandpermissions

1. Zandi-Nejad, K., Eddy, A.A., Glassock, R.J. & Brenner, B.M. Why is proteinuria an ominous biomarker of progressive kidney disease? *Kidney Int. Suppl.* **66**, S76–S89 (2004).
2. Kerjaschki, D. *et al.* A β1-integrin receptor for fibronectin in human kidney glomeruli. *Am. J. Pathol.* **134**, 481–489 (1989).
3. Kreidberg, J.A. *et al.* α3β1 integrin has a crucial role in kidney and lung organogenesis. *Development* **122**, 3537–3547 (1996).
4. Regele, H.M. *et al.* Glomerular expression of dystroglycans is reduced in minimal change nephrosis but not in focal segmental glomerulosclerosis. *J. Am. Soc. Nephrol.* **11**, 403–412 (2000).
5. Reiser, J., Kriz, W., Kretzler, M. & Mundel, P. The glomerular slit diaphragm is a modified adherens junction. *J. Am. Soc. Nephrol.* **11**, 1–8 (2000).
6. Faul, C., Asanuma, K., Yanagida-Asanuma, E., Kim, K. & Mundel, P. Actin up: regulation of podocyte structure and function by components of the actin cytoskeleton. *Trends Cell Biol.* **17**, 428–437 (2007).
7. Tryggvason, K., Patrakka, J. & Wartiovaara, J. Hereditary proteinuria syndromes and mechanisms of proteinuria. *N. Engl. J. Med.* **354**, 1387–1401 (2006).
8. Sever, S. *et al.* Proteolytic processing of dynamin by cytoplasmic cathepsin L is a mechanism for proteinuric kidney disease. *J. Clin. Invest.* **117**, 2095–2104 (2007).
9. Reiser, J. *et al.* Induction of B7-1 in podocytes is associated with nephrotic syndrome. *J. Clin. Invest.* **113**, 1390–1397 (2004).
10. Reiser, J. *et al.* Podocyte migration during nephrotic syndrome requires a coordinated interplay between cathepsin L and α3 integrin. *J. Biol. Chem.* **279**, 34827–34832 (2004).
11. Asanuma, K. *et al.* Synaptopodin orchestrates actin organization and cell motility via regulation of RhoA signalling. *Nat. Cell Biol.* **8**, 485–491 (2006).
12. Moeller, M.J. *et al.* Podocytes populate cellular crescents in a murine model of inflammatory glomerulonephritis. *J. Am. Soc. Nephrol.* **15**, 61–67 (2004).
13. Seiler, M.W., Venkatachalam, M.A. & Cotran, R.S. Glomerular epithelium: structural alterations induced by polycations. *Science* **189**, 390–393 (1975).
14. Van Den Berg, J.G., Van Den Bergh Weerman, M.A., Assmann, K.J.M., Weening, J.J. & Florquin, S. Podocyte foot process effacement is not correlated with the level of proteinuria in human glomerulopathies. *Kidney Int.* **66**, 1901–1906 (2004).
15. Gadea, G., de Toledo, M., Anguille, C. & Roux, P. Loss of p53 promotes RhoA-ROCK–dependent cell migration and invasion in 3D matrices. *J. Cell Biol.* **178**, 23–30 (2007).
16. Wei, Y. *et al.* Regulation of integrin function by the urokinase receptor. *Science* **273**, 1551–1555 (1996).
17. Blasi, F. & Carmeliet, P. uPAR: a versatile signalling orchestrator. *Nat. Rev. Mol. Cell Biol.* **3**, 932–943 (2002).
18. Alfano, M., Sidenius, N., Panzeri, B., Blasi, F. & Poli, G. Urokinase-urokinase receptor interaction mediates an inhibitory signal for HIV-1 replication. *Proc. Natl. Acad. Sci. USA* **99**, 8862–8867 (2002).
19. Wei, Y. *et al.* Identification of the urokinase receptor as an adhesion receptor for vitronectin. *J. Biol. Chem.* **269**, 32380–32388 (1994).
20. Madsen, C.D., Ferraris, G.M., Andolfo, A., Cunningham, O. & Sidenius, N. uPAR-induced cell adhesion and migration: vitronectin provides the key. *J. Cell Biol.* **177**, 927–939 (2007).
21. Dewerchin, M. *et al.* Generation and characterization of urokinase receptor–deficient mice. *J. Clin. Invest.* **97**, 870–878 (1996).
22. Carmeliet, P. *et al.* Biological effects of disruption of the tissue-type plasminogen activator, urokinase-type plasminogen activator, and plasminogen activator inhibitor-1 genes in mice. *Ann. NY Acad. Sci.* **748**, 367–382 (1995).
23. Zheng, X., Saunders, T.L., Camper, S.A., Samuelson, L.C. & Ginsburg, D. Vitronectin is not essential for normal mammalian development and fertility. *Proc. Natl. Acad. Sci. USA* **92**, 12426–12430 (1995).
24. Hodivala-Dilke, K.M. β3-integrin–deficient mice are a model for Glanzmann thrombasthenia showing placental defects and reduced survival. *J. Clin. Invest.* **103**, 229–238 (1999).
25. Simons, K. & Toomre, D. Lipid rafts and signal transduction. *Nat. Rev. Mol. Cell Biol.* **1**, 31–39 (2000).
26. Schmid, H. *et al.* Validation of endogenous controls for gene expression analysis in microdissected human renal biopsies. *Kidney Int.* **64**, 356–360 (2003).
27. Nakamura, T., Ebihara, I., Shirato, I., Tomino, Y. & Koide, H. Modulation of basement membrane component gene expression in glomeruli of aminonucleoside nephrosis. *Lab. Invest.* **64**, 640–647 (1991).
28. Kelley, V.E. & Cavallo, T. An ultrastructural study of the glomerular slit diaphragm in New Zealand black/white mice. *Lab. Invest.* **35**, 213–220 (1976).
29. Mundel, P. *et al.* Synaptopodin: an actin-associated protein in telencephalic dendrites and renal podocytes. *J. Cell Biol.* **139**, 193–204 (1997).
30. Shankland, S.J., Pippin, J.W., Reiser, J. & Mundel, P. Podocytes in culture: past, present, and future. *Kidney Int.* **72**, 26–36 (2007).
31. Mauer, S.M. *et al.* Effects of kidney and pancreas transplantation on streptozotocin-induced malignant kidney tumors in rats. *Cancer Res.* **34**, 1643–1645 (1974).
32. Mayer, G., Boileau, G. & Bendayan, M. Furin interacts with proMT1-MMP and integrin αv at specialized domains of renal cell plasma membrane. *J. Cell Sci.* **116**, 1763–1773 (2003).
33. Moeller, M.J., Sanden, S.K., Soofi, A., Wiggins, R.C. & Holzman, L.B. Podocyte-specific expression of cre recombinase in transgenic mice. *Genesis* **35**, 39–42 (2003).
34. Velasco, B. *et al.* Vascular gene transfer driven by endoglin and ICAM-2 endothelial-specific promoters. *Gene Ther.* **8**, 897–904 (2001).
35. Zeisberg, E.M. *et al.* Endothelial-to-mesenchymal transition contributes to cardiac fibrosis. *Nat. Med.* **13**, 952–961 (2007).
36. Arnaout, M.A., Mahalingam, B. & Xiong, J.P. Integrin structure, allostery, and bidirectional signaling. *Annu. Rev. Cell Dev. Biol.* **21**, 381–410 (2005).
37. Chaurasia, P. *et al.* A region in urokinase plasminogen receptor domain III controlling a functional association with α5β1 integrin and tumor growth. *J. Biol. Chem.* **281**, 14852–14863 (2006).
38. Wei, Y. *et al.* Urokinase receptors are required for α5β1 integrin–mediated signaling in tumor cells. *J. Biol. Chem.* **282**, 3929–3939 (2007).
39. Degryse, B., Resnati, M., Czekay, R.P., Loskutoff, D.J. & Blasi, F. Domain 2 of the urokinase receptor contains an integrin-interacting epitope with intrinsic signaling activity: generation of a new integrin inhibitor. *J. Biol. Chem.* **280**, 24792–24803 (2005).
40. Pelletier, A.J., Kunicki, T. & Quaranta, V. Activation of the integrin αvβ3 involves a discrete cation-binding site that regulates conformation. *J. Biol. Chem.* **271**, 1364–1370 (1996).
41. Honda, S. *et al.* Topography of ligand-induced binding sites, including a novel cation-sensitive epitope (AP5) at the amino terminus, of the human integrin β3 subunit. *J. Biol. Chem.* **270**, 11947–11954 (1995).
42. Dormond, O., Foletti, A., Paroz, C. & Ruegg, C. NSAIDs inhibit αvβ3 integrin–mediated and Cdc42/Rac-dependent endothelial-cell spreading, migration and angiogenesis. *Nat. Med.* **7**, 1041–1047 (2001).
43. Cai, W. & Chen, X. Anti-angiogenic cancer therapy based on integrin αvβ3 antagonism. *Anticancer Agents Med. Chem.* **6**, 407–428 (2006).
44. Schwarz, K. *et al.* Podocin, a raft-associated component of the glomerular slit diaphragm, interacts with CD2AP and nephrin. *J. Clin. Invest.* **108**, 1621–1629 (2001).
45. Keller, P. & Simons, K. Cholesterol is required for surface transport of influenza virus hemagglutinin. *J. Cell Biol.* **140**, 1357–1367 (1998).
46. Butta, N. *et al.* Disruption of the β3 663–687 disulfide bridge confers constitutive activity to beta3 integrins. *Blood* **102**, 2491–2497 (2003).
47. Pampori, N. *et al.* Mechanisms and consequences of affinity modulation of integrin αvβ3 detected with a novel patch-engineered monovalent ligand. *J. Biol. Chem.* **274**, 21609–21616 (1999).
48. Hughes, P.E. *et al.* Breaking the integrin hinge. A defined structural constraint regulates integrin signaling. *J. Biol. Chem.* **271**, 6571–6574 (1996).
49. de Jong, P.E. & Brenner, B.M. From secondary to primary prevention of progressive renal disease: the case for screening for albuminuria. *Kidney Int.* **66**, 2109–2118 (2004).
50. Silberman, S., Janulis, M. & Schultz, R.M. Characterization of downstream Ras signals that induce alternative protease-development invasive phenotypes. *J. Biol. Chem.* **272**, 5927–5935 (1997).
51. Gugliucci, A. & Bendayan, M. Reaction of advanced glycation endproducts with renal tissue from normal and streptozotocin-induced diabetic rats: an ultrastructural study using colloidal gold cytochemistry. *J. Histochem. Cytochem.* **43**, 591–600 (1995).